**Journal of Magnetics** 11(2), 90-94 (2006)

# A Finite-element Method Analysis of Electromagnetic Noise Absorption in a Coplanar Transmission Line Integrated with a Magnetic Film

**Jae Cheon Sohn, Suk Hee Han, and Sang Ho Lim[1]***

*Nano Device Research Center, Korea Institute of Science and Technology, P. O. Box 131, Cheongryang, Seoul 130-650, Korea*
*[1]Division of Materials Science and Engineering, Korea University, Seoul 136-713, Korea*

(Received 26 May 2006)

**A finite-element method is used to analyze loss generation and electromagnetic noise absorption characteristics of a coplanar waveguide transmission line integrated with a magnetic thin film. Parameters used in the analysis are the electrical resistivity of the magnetic layer and the thickness of both magnetic and insulating layers. The results indicate that L-C resonance is the main loss mechanism of the electromagnetic noise absorption.**

**Key words :** electromagnetic noise absorption, coplanar waveguide transmission line, magnetic thin film, finite-element method, L-C resonance

## 1. Introduction

Many studies have been performed to apply soft magnetic materials to electromagnetic noise absorbers in the GHz frequency band. However, the main loss mechanism causing electromagnetic noise absorption has not been cleared up yet. Some researchers reported that the ferromagnetic resonance (FMR) was the main loss mechanism for electromagnetic noise absorption [1-4]. However, our previous results indicated that L-C resonance is responsible for the main loss mechanism, occurring through a coupling of inductance of a magnetic film and non-distributed capacitance of a dielectric layer [5]. One piece of evidence is the shift of the noise absorption peak toward a low frequency band with increasing thickness of a magnetic film [5]. As the magnetic film thickness increases, the inductance (L) increases and hence L-C resonance frequency moves toward a low frequency band. An opposite trend should be observed if FMR is the main loss mechanism; as the magnetic film thickness increases, the shape anisotropy increases, resulting in increased FRM FMR frequency. So, the main purpose of the present study is to test our previous experimental results [5] by using a commercial high frequency simulation program (HFSS ver. 9.2.1).

*Corresponding author: Tel: +82-2-3290-3285,
Fax: +82-2-928-3584, e-mail: sangholim@korea.ac.kr

## 2. Finite Element Method Analysis

The finite element method (FEM) is a numerical technique for efficiently solving problems which are described by partial differential equations. A domain of interest is represented as an assembly of finite elements. Approximating functions in finite elements are determined in terms of nodal values of a physical field which is sought. A continuous physical problem is transformed into a discretized finite element problem with unknown nodal values. To discretize a continuum is the first step in a FEM analysis. And it is to divide a solution region into finite elements. The finite element models for practical analysis can contain tens of thousands or even hundreds of thousands degree of freedom. It is not possible to create such meshes manually. Mesh generator is a software tool, which divides the solution domain into many sub-domains, finite elements.

Let us consider a three-dimensional coplanar transmission line subjected to a radio frequency power. In the GHz frequency range, not only the eddy currents, but also the displacement currents are important to describe the energy loss behavior. In this study, we used a 3D FEM based on the complete set of Maxwell's equations, including the displacement current term and the continuity equation of current. From Faraday's law and Gauss' law for magnetic fields, the electric scalar potential $\phi$ and the magnetic vector potential $\overline{A}$ are defined as follows;

$$\vec{E}=-\frac{\partial \vec{A}}{\partial t}-grad\phi \quad (1)$$

$$\vec{B}=rot\vec{A}. \quad (2)$$

The basic equations for this FEM analysis for time-harmonic magnetic vector potential and electric scalar potential in the absence of spatial charges are;

$$rot\frac{1}{\mu}(rot\vec{A})-(\sigma+j\omega\varepsilon)(j\omega\vec{A}+grad\phi)=0 \quad (3)$$

$$div(\sigma+j\omega\varepsilon)(j\omega\vec{A}+grad\phi)=0 \quad (4)$$

where $\mu$, $\varepsilon$ and $\sigma$ are permeability, permittivity and conductivity, respectively. The permeability $\mu$ is given as a complex value. The magnetic vector potentials and electric scalar potentials are also obtained as complex values.

The detailed structure of the simulated device is shown in Figs. 1(a) and (b) for an overall schematic and the cross-section, respectively. Following the Muller and Hillberg equations [6], a coplanar transmission line with a characteristic impedance of 50 Ω was designed for a signal line width of 50 $\mu$m and a thickness of 3 $\mu$m on a #7059 Corning glass substrate. Material parameters for simulation are listed in Table 1. For device simulation, it was assumed that the permittivity ($\varepsilon_r$=4) of $SiO_2$ film was independent on the frequency, the volume resistivity was high enough, and the loss tangent was negligibly small. The transmission coefficient $S_{21}$ and reflection coefficient $S_{11}$ were calculated using Eqs. (5)~(8);

$$S_{21}[dB]=20\log\frac{V_{o\_\max}}{V_{i\_\max}} \quad (5)$$

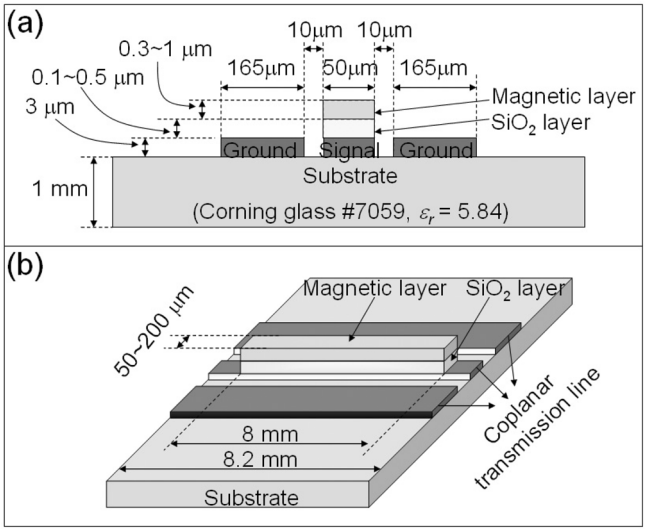


**Fig. 1.** The device structure considered in the simulation, showing (a) an overall schematic and (b) the cross-section.

**Table 1.** Material parameters used in the simulation; relative permittivity ($\varepsilon_r$), relative permeability ($\mu_r$), bulk conductivity ($\sigma_B$), dielectric loss tangent (tan$\delta_D$) and magnetic loss tangent (tan$\delta_M$), and the Lande $g$ factor.

| Material | Parameters | | | | | |
|---|---|---|---|---|---|---|
| | $\varepsilon_r$ | $\mu_r$ | $\sigma_B$ ($\Omega^{-1}$cm$^{-1}$) | tan$\delta_D$ | tan$\delta_M$ | Lande $g$ factor |
| Corning glass #7059 | 5.75 | 1 | 0 | 0 | 0 | 0 |
| Cu | 1 | 0.999991 | $5.8\times10^9$ | 0 | 0 | 0 |
| $SiO_2$ | 4 | 1 | 0 | 0 | 0 | 2 |
| Co-Fe-Al-O | 1.2 | 500~1000 | $10^3$~$10^4$ | 0 | 0 | 2 |

$$S_{21}[\deg]=\phi_{V(out\_\max)}-\phi_{V(in\_\max)} \quad (6)$$

$$S_{11}[dB]=20\log\frac{V_{r\_\max}}{V_{i\_\max}} \quad (7)$$

$$S_{11}[\deg]=\phi_{V(ref\_\max)}-\phi_{V(in\_\max)} \quad (8)$$

where $V_{o\_\max}$ is the magnitude of each maximum peak of output voltage wave and $V_{i\_\max}$ is that of input voltage wave. Some portion of the input signal toward the output port is always reflected from the interfacial boundaries between the coplanar transmission line and the upper layer and returns toward the input port. $V_{r\_\max}$ is the magnitude of each maximum peak of this reflected voltage signal. $\phi_{V(out\_\max)}$, $\phi_{V(in\_\max)}$ and $\phi_{V(ref\_\max)}$ are the phases of each maximum peak of the input, output and reflected signals, respectively. The input impedance $Z_{11}$ is calculated by using Eq. 9;

$$Z_{in}=Z_0\frac{1+S_{11}}{1-S_{11}} \quad (9)$$

where $Z_0$, the characteristic impedance, is set to 50 Ω.

## 3. Results and Discussion

Fig. 2 shows the frequency dependence of the transmitted scattering parameters ($S_{21}$) of the simulated structure. In the simulation, the effect of the FMR loss on the signal attenuation is also examined. The thickness, width and length of the magnetic thin film are 1 $\mu$m, 200 $\mu$m and 8 mm, respectively, while the values of resistivity ($\rho$), saturated magnetization ($4\pi M_S$) and anisotropy field ($H_K$) are fixed at 300 $\mu\Omega$cm, 15 kG and 15 Oe, respectively. The FMR frequency of the present magnetic thin film, which can be estimated by using the Landau-Lifshitz-Gilbert equation, is 1.33 GHz at the given values of $\rho$ and $4\pi M_S$. This resonance frequency is "intrinsic" in the sense that the "extrinsic" shape anisotropy is not taken into account in the calculation. The thickness of the insulating

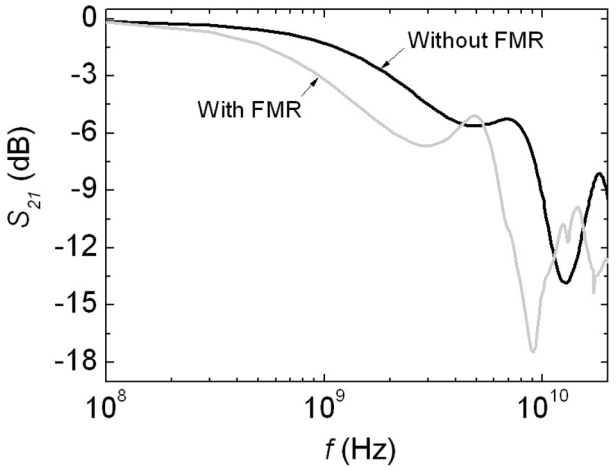


**Fig. 2.** The frequency dependence of the transmitted scattering parameters ($S_{21}$). Two sets of results are shown; one under the assumption of no FMR in the magnetic thin film (indicated by a thick solid line) and the other in the presence of FMR at 1.33 GHz (denoted by a thin dotted line).

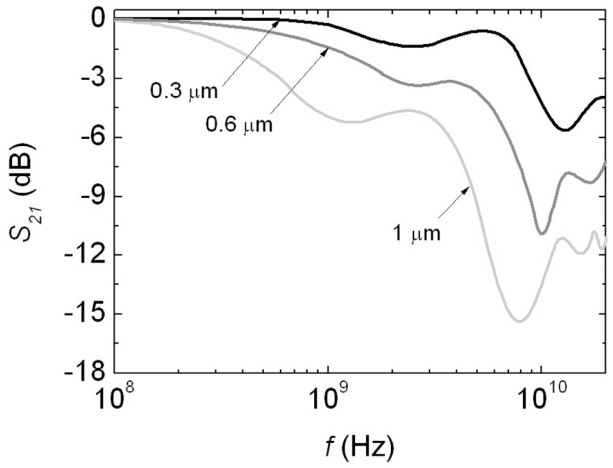


**Fig. 3.** The frequency dependence of $S_{21}$ at various magnetic thicknesses of 0.3 $\mu$m, 0.6 $\mu$m and 1 mm.

$SiO_2$ layer disposed between the magnetic layer and the coplanar transmission line is 0.5 $\mu$m. The simulated frequency range is 0.1~20 GHz. Two sets of results are shown in Fig. 2; one set of results are obtained under the assumption of no FMR in the magnetic thin film (indicated by a thick solid line) and the other calculated in the presence of FMR at 1.33 GHz (denoted by a thin dotted line). In the former case of no FMR condition, the parameters of permeability, permittivity, magnetic loss tangent and dielectric loss tangent, which are usually frequency dependent, are also assumed to be independent of frequency. In the latter case, however, the frequency dependency was considered for the frequency dependent parameters. As FMR is made to occur in the magnetic thin film, the frequency of the absorption peak (which is indicated by the dip of $S_{21}$) decreases from 13 GHz to 9 GHz while the magnitude of $S_{21}$ increases from −14 dB to −17.5 dB. One important point from the comparison is that the main absorption peaks are far higher than the intrinsic FMR frequency. Furthermore, there is no detectable change in the results near the FMR frequency. This may provide evidence that the FMR loss is not the main loss mechanism for electromagnetic noise absorption. The role of the FMR loss is to change the frequency and magnitude of the absorption peak, although the reason for this is not clearly understood.

The results for the frequency dependence of $S_{21}$ at various magnetic thicknesses are shown in Fig. 3, where the thicknesses of the magnetic layer considered are 0.3 $\mu$m, 0.6 $\mu$m and 1 $\mu$m, while its width and length are fixed at 50 $\mu$m and 8 mm, respectively. The thickness of $SiO_2$ insulating layer is fixed at 0.1 $\mu$m. The values of $\rho$, $4\pi M_S$ and $H_K$ of the magnetic layer are fixed at 100 $\mu\Omega$cm, 15 kG and 15 Oe, respectively. The simulation is done without considering FMR. A progressive change in the noise absorption peak occurs with the thickness change. As the thickness of the magnetic layer increases from 0.3 $\mu$m to 0.6 $\mu$m, the noise absorption peak decreases from 12.8 GHz to 10.5 GHz, and the magnitude of $S_{21}$ also decreases from −6 dB to −10.5 dB. At the largest thickness of 1 $\mu$m, the frequency and magnitude respectively are 8.2 GHz and −16 dB. The reason for this change is closely related with the thickness dependence of inductance of the magnetic layer and the L-C resonance frequency. The inductance of a magnetic body is proportional to its volume. The frequency where L-C resonance occurs is calculated as follows;

$$f_{L-C}=\frac{1}{2\pi\sqrt{LC}} \tag{10}$$

As the thickness of the magnetic layer increases, the inductance increases and the frequency of L-C resonance moves toward the low frequency band. In this case, the capacitance, in its distributed form, also exists because the distributed capacitor is formed by the $SiO_2$ layer ($\varepsilon_r$=4). So, it is safe to mention that the noise absorption peak in this simulation occurs by L-C resonance.

The results for the frequency dependence of $S_{21}$ at various thicknesses of the $SiO_2$ insulating layer are shown in Fig. 4. The thicknesses of the insulating layer considered are 0.1 $\mu$m, 0.3 $\mu$m and 0.5 $\mu$m. The thickness, width and length of the magnetic layer are respectively fixed at 1 $\mu$m, 50 $\mu$m and 8 mm. The values of $\rho$, $4\pi M_S$ and $H_K$ of the magnetic layer are fixed at 500 $\mu\Omega$cm, 15 kG and 30 Oe, respectively. The simulation is done

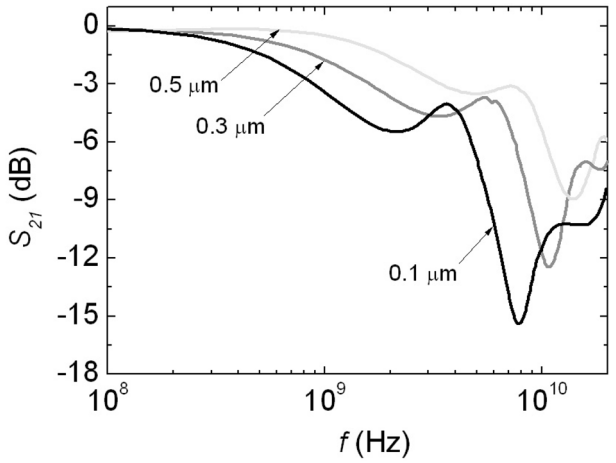


**Fig. 4.** The frequency dependence of $S_{21}$ at various $SiO_2$ thicknesses of 0.1 $\mu$m, 0.3 $\mu$m and 0.5 $\mu$m.

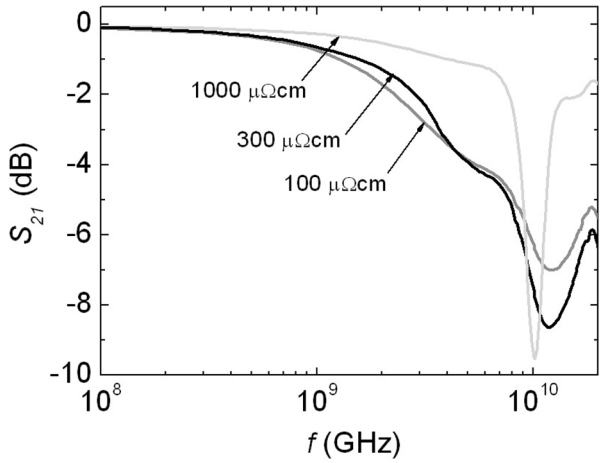


**Fig. 5.** The frequency dependence of $S_{21}$ at various values of electrical resistivity ($\rho$) of the magnetic layer: 100 $\mu\Omega$cm, 300 $\mu\Omega$cm and 1000 $\mu\Omega$cm.

without considering FMR. When the $SiO_2$ layer thickness is 0.1 $\mu$m, the noise absorption peak occurs at 7.8 GHz and the magnitude of $S_{21}$ is −15.5 dB. As the thickness increases, the frequency of the absorption peak moves toward the high frequency band while the magnitude decreases. At the thickness of 0.3 $\mu$m, the resonance frequency and magnitude of $S_{21}$ respectively are 10.5 GHz and −12.7 dB and, at the thickness of 0.5 $\mu$m, they are respectively 14 GHz and −9 dB. This change with the thickness of the $SiO_2$ layer is closely related with the capacitance of the $SiO_2$ layer and L-C resonance. The insulating $SiO_2$ layer is located between the magnetic layer and the Cu transmission line and this structure forms a capacitor. This is because the magnetic layer and the Cu transmission line act as metal electrodes. Accordingly, this structure generates the distributed capacitance in the high frequency region. The capacitance of a dielectric substance is the function which is usually inversely proportional to its thickness. As the thickness of the dielectric substance increases, the capacitance decreases and, according to Eq. 10, the L-C resonance frequency increases. Similarly to the results shown in Fig. 3, the noise absorption peak occurs due to L-C resonance which occurs by the coupling between the distributed inductance of magnetic layer and the distributed capacitance of $SiO_2$ layer.

The results for the frequency dependence of $S_{21}$ are shown in Fig. 5 at various values of electrical resistivity ($\rho$) of the magnetic layer: 100 $\mu\Omega$cm, 300 $\mu\Omega$cm and 1000 $\mu\Omega$cm. The thickness, width and length of the magnetic layer are fixed at 0.5 $\mu$m, 50 $\mu$m and 8 mm, respectively, while the values of $4\pi M_S$ and $H_K$ are respectively 15 kG and 15 Oe. The thickness of $SiO_2$ layer is fixed at 0.1 $\mu$m. Again, the simulation is done without considering FMR. When the value of $\rho$ is 1000 $\mu\Omega$cm, the noise absorption peak occurs at 10 GHz and the magnitude of $S_{21}$ is −10 dB. As the resistivity decreases below 1000 $\mu\Omega$cm, the frequency at which the noise absorption begins to occur moves toward the low frequency range. On the contrary, the frequency of the noise absorption peak moves toward the high frequency range, although the change is small. In this case, the magnitude of the absorption peak decreases. At $\rho$ = 1000 $\mu\Omega$cm, the noise absorption characteristics typical of a band stop filter are seen; at a level of −3 dB which is usually taken to be the boundary of a weak signal transmittance, the noise absorption starts at 8 GHz and ends at 12 GHz. At $\rho$ = 300 $\mu\Omega$cm, the noise absorption starts at 3.66 GHz and the absorption peak occurs at 11 GHz with a magnitude of −9 dB. At $\rho$ = 100 $\mu\Omega$cm, the noise absorption starts at 3.36 GHz and the absorption peak occurs at 12 GHz with a magnitude of −7.23 dB. Obviously, the change of the noise absorption frequency as a function of the resistivity is related with the eddy current effect. The eddy current is high at high frequencies and it is low at high values of resistivity, although detailed relationship among them is geometry dependent, making it difficult to calculate. However, it is expected that the magnitude of eddy current itself does not affect significantly the noise absorption characteristics; instead, its effect is indirect through the change of the permeability of the magnetic thin film and hence the inductance. The large eddy current loss will decrease the permeability of the magnetic substance in the high frequency region. Because the inductance of the magnetic substance is the function of its permeability, the inductance decreases as the permeability decreases. So, the L-C resonance frequency increases and

the frequency of the noise absorption peak shifts toward the high frequency band.

## 4. Conclusions

A finite-element method using a commercial simulation package (HFSS version 9.2.1) was applied to analyze the loss generation and electromagnetic noise absorption characteristics of a coplanar waveguide transmission line integrated with a magnetic thin film. The variation of electromagnetic noise absorption characteristics is examined with the thickness of both magnetic and insulating layers and the electrical resistivity of the magnetic layer. As the thickness of the magnetic layer increases, the frequency of the noise absorption peak moves toward the low frequency band, due to the increased inductance and hence the reduced L-C resonance frequency. The effects of the thickness of the $SiO_2$ insulating layer can be explained similarly; as the thickness of the insulating layer increases, the frequency of the noise absorption peak moves toward the low frequency band, due to the decreased capacitance and hence the increased L-C resonance frequency. The noise absorption bandwidth increases slightly as the electrical resistivity of the magnetic layer decreases, possibly due to the decreased permeability of the magnetic layer. No significant change is observed between the results obtained by considering FMR and those without FMR. The present simulation results indicate that L-C resonance is the main loss mechanism for the electromagnetic noise absorption, with minor contributions from FMR and eddy currents.

## Acknowledgments

This work is supported by a Korea University Grant.

## References

[1] M. Yamaguchi, Ki-Hyeon Kim, Takashi Kuribara, and Ken-Ichi Arai, *Thin-Film RF Noise Suppressor Integrated in a Transmission Line.* IEEE Trans. Magn. **37**(5), 3183-3185 (2002).

[2] K. H. Kim, M. Yamaguchi, K. I. Arai, H. Nagura, and S. Ohnuma, J. Appl. Phys., *Effect of Radio-Frequency Noise Suppression on the Coplanar Transmission Line Using Soft Magnetic Thin Films.* J. Appl. Phys. **93**(10), 8002-8004 (2003).

[3] K. H. Kim, M. Yamaguchi, K. I. Arai, N. Matsushita, and M. Abe, *Application of Spin Sprayed Ferrite Films on Coplanar Transmission Line for RF Noise Suppression.* Trans. Magn. Soc. Japan **3**(4), 133-136 (2003).

[4] K. H. Kim, M. Yamaguchi, S. Ikeda, and K. I. Arai, *Modeling for RF Noise Suppressor Using a Magnetic Film on Coplanar Transmission Line.* IEEE Trans. Magn. **39**(5), 3031-3033 (2003).

[5] J. C. Sohn, S. H. Lim, S. H. Han, and M. Yamaguchi, *RF Integrated Electromagnetic Noise filters Incorporated with Nanogranular $Co_{41}Fe_{38}Al_{13}O_8$ Soft Magnetic Thin Films on Coplanar Transmission Line.* J. Magnetics **10**(4), 163-170 (2005).

[6] B. C. Wadell, *Transmission Line Design Handbook.* Artech House, Massachusetts (1991), Chap. 3.